Chinese Journal of Electronics
Vol.20, No.2, Apr. 2011

Data Center Local Thermal Management Based on Thermal Cameras Networks*

LIU Hang[1], LEE Eun Kyung[2], POMPILI Dario[2] and KONG Xiangwei[1]

(1.*School of Information and Communication Engineering, Dalian University of Technology, Dalian 116023, China*)

(2.*Department of Electrical and Computer Engineering, the State University of New Jersey, NJ, Rutgers, 08854, USA*)

Abstract — Global data center capacity is growing rapidly, consuming more financial resources and emitting more greenhouse gases. A significant portion of typical data centers energy consumption can be apportioned to the cooling infrastructure. In this paper, we proposed a Thermal camera network (TCN) to improve utilization of the cooling infrastructure. It can cool the hotspots intelligently instead of the whole data center. A TCN is composed of multiple thermal cameras and actors, which can wirelessly communicate with each other. Actors will cool the region where hotspots appear as soon as thermal cameras locate the hotspots. In that way, the TCN can save substantial energy in some meaning. In addition, this paper addresses the method of cooperatively detection and formulates the coordinates of the hotspot located by multiple thermal cameras.

Key words — Data center thermal management, Thermal image, Thermal cameras, Sensor networks, Computer vision, Energy saving.

I. Introduction

Data centers exhibit high power density and heat generation. In the near future, increase in the computational performance will lead electronic cabinets to house high performance chips with heat fluxes approaching 100W/cm^2[1]. High temperature decreases the reliability of the affected components to the point that they start to behave unpredictably or fail altogether. Thus energy consumption and temperature management have emerged as key design challenges in creating new data center architectures[2−4]. For a large-scale data center, the annual energy cost can be up to millions of dollars, with the cooling cost being at least half of the total energy cost[5]. Although recently built data centers exhibit better cooling efficiency, cooling energy consumption is still a significant portion of the total data center energy consumption[6]. A key cause is that although these cooling systems can effectively control the average temperature of the whole data center and save substantial energy by controlling inlet temperature, thermal imbalances interfere with efficient cooling operation and unexpected localized high temperature regions, called as hotspots, still exist. Hotspots are a ubiquitous problem in air-cooled data centers, and drive the environmental control system to work much harder to ensure that no server is fed hot air (*i.e.*, air at a temperature greater than the target threshold)[7]. Hotspots may be generated by several factors that are hot air at the top sections of computer racks, poor design of the cooling infrastructure or air distribution system, failed fans or air conditioners, accidental overload due to hardware upgrades, or degraded operation during brownouts[8]. These hotspots may go undetected for a long time, generating corresponding losses in reliability and, when components eventually fail, performance.

Thus, a Thermal camera network (TCN) is proposed in this paper. It is a kind of Wireless sensor and actor networks (WSANs)[9,10] which are composed of heterogeneous devices referred to as sensors and actors. The sensors in TCNs are intelligent pan-tilt thermal camera nodes. These nodes which are sparsely deployed can obtain and process thermal images and wirelessly communicate with each other. After they detect and locate a hotspot cooperatively, they transmit the coordinates of the hotspot to actors. Actors will cool the region where the hotspot appears but not the whole data center. Actors can adopt a lot of ways to perform this action. For example, they can control cooling devices to selectively cool or perform job migration[11,12], etc. The availability of inexpensive and miniature hardware promotes the development of TCNs.

The remainder of this paper is organized as follows. In Section II, the system hardware is described. Section III solves several problems about detecting and locating the hotspot with the TCN. Because of sparse deployment of the cameras, their cooperation is essential to maximize efficiency and effectiveness. So we propose a method to cooperatively detect and locate hotspots with the TCN. In Section IV, several experimental results are presented and discussed, and finally Section V summarizes and provides concluding statements.

II. System Hardware

The TCN consists of several thermal camera nodes deployed sparsely, represented as $C_1, C_2, \cdots, C_N$, where N is the

*Manuscript Received Apr. 2010; Accepted June 2010.

number of the cameras, and some actor nodes. The powerful processing board (Imote2, Crossbow) connected to a thermal camera is used for image processing and IEEE 802.15.4 is used for the radio. These nodes can locate and cool the hotspot collaboratively with the ability to compute and communicate.

The thermal camera has a temperature measurement range of -40 to $80°$C with temperature resolution less than $0.1°$C. It has a low resolution uncooled microbolometer detector, and it can display thermal images of $W \times H$ pixels ($W = 320$ and $H = 240$). The other internal parameters are focal length $F = \|Co\|$, horizontal angle $\alpha^h = \angle ACB$ and vertical angle $\alpha^v = \angle DCE$ of view, and principal point o, the coordinate of o in the thermal image $p(o) = [W/2, H/2]^T$ (Fig.1(a)). These thermal cameras can pan and tilt rotate automatically. We assume the horizontal and vertical angle of optical axis, β^h and β^v (Fig.1(b)), and the location of the camera, $P(C) = [X_C, Y_C, Z_C]^T$, are known. In this paper, $p(q)$ denotes the coordinates of the point q in the thermal image, namely $p(q) = [x_q, y_q]^T$, and $P(Q)$ denotes the world coordinates of the point Q, namely $P(Q) = [X_Q, Y_Q, Z_Q]^T$.

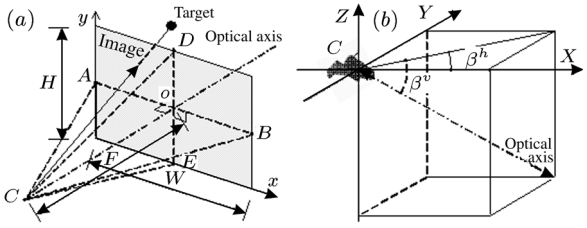

Fig. 1. Parameters of the thermal camera

III. Detecting and Locating

1. Cooperatively detecting

Because of restriction of the small angle of view of the camera, one camera cannot see the full extent of the monitored area, even though cameras can pan and tilt automatically. An appropriate cooperatively detecting mechanism can accelerate detecting hotspots with a TCN. Since hotspots can levitate in the air, the TCN must cover the whole 3D space but not only the floor.

According to the principle of computational stereo, the world coordinates of a point can be calculated by two or more cameras. The precondition for cooperative calculation of a hotspot center is two or more cameras can find the same hotspot. If a camera, C_i, finds a hotspot, H, from a thermal image, it will transmit the information of H to other cameras. Then these cameras will detect H according to the information. Because of restriction of the small angle of view, it will take a long time that a camera scans the whole 3D space and then compares the hotspots found by itself to H to choose the corresponding spot. Thus we propose a method to simplify cooperatively detecting mode from 3D to 2D.

If C_i finds a hotspot H, it will calculate the straight line $\overleftrightarrow{C_iH}$ that passes C_i and H at first. The method of calculating is as follows.

At first, C_i estimates the 2D coordinates of the projection of the hotspot center in the thermal image, namely $p(h)$. Since the intensity values of the thermal image are the temperature values, we use isotherms to estimate $p(h)$ in the thermal images. The isotherm is a line connecting points of equal temperature. We define the edge of the hotspot in the thermal image is the isotherm at warning temperature. Let ξ denote the area of the hotspot in the image, and function $T(x, y)$ denote the temperature at $[x, y]^T$ in the image. So the coordinates of the hotspot center in the image, $p(h) = [x_h, y_h]^T$, is defined as follows:

$$p(h) = \begin{bmatrix} x_h \\ y_h \end{bmatrix} = \frac{1}{\sum_{[x,y]\in\xi} T(x,y)} \begin{bmatrix} \sum_{[x,y]\in\xi} xT(x,y) \\ \sum_{[x,y]\in\xi} yT(x,y) \end{bmatrix} \quad (1)$$

Since the intersection of the straight line $\overleftrightarrow{C_iH}$ and the image plane is h in the image, $\overleftrightarrow{C_iH}$ and $\overleftrightarrow{C_ih}$ are the same straight line. So the horizontal and vertical angle between $\overleftrightarrow{C_iH}$ and the optical axis $\overleftrightarrow{C_io}$ are:

$$\begin{cases} \gamma_i^h = \arctan((x_h - W/2)/F) \\ \gamma_i^v = \arctan((y_h - H/2)/F) \end{cases} \quad (2)$$

So the horizontal and vertical angle of $\overleftrightarrow{C_iH}$ are

$$\begin{cases} \beta^h_{\overleftrightarrow{C_iH}} = \beta_i^h - \gamma_i^h \\ \beta^v_{\overleftrightarrow{C_iH}} = \beta_i^v - \gamma_i^v \end{cases} \quad (3)$$

respectively. Thus, $\overleftrightarrow{C_iH}$ can be described as

$$\overleftrightarrow{C_iH} = \boldsymbol{l}_i \cdot t + P(C_i) \quad (4)$$

where $\boldsymbol{l}_i$ is the direction vector of $\overleftrightarrow{C_iH}$,

$$\boldsymbol{l}_i = \begin{bmatrix} X_{\boldsymbol{l}_i} \\ Y_{\boldsymbol{l}_i} \\ Z_{\boldsymbol{l}_i} \end{bmatrix} = \begin{bmatrix} \cos\beta^v_{\overleftrightarrow{C_iH}} \cdot \cos\beta^h_{\overleftrightarrow{C_iH}} \\ \cos\beta^v_{\overleftrightarrow{C_iH}} \cdot \sin\beta^h_{\overleftrightarrow{C_iH}} \\ -\sin\beta^v_{\overleftrightarrow{C_iH}} \end{bmatrix} \quad (5)$$

Then C_i transmits relevant data to the cameras around. The data includes the location of C_i and $\boldsymbol{l}_i$.

If camera C_j receives the data from C_i, it starts to calculate the distance between itself to $\overleftrightarrow{C_iH}$, namely $\|C_j, \overleftrightarrow{C_iH}\|$. if $TH_1 < \|C_j, \overleftrightarrow{C_iH}\| < TH_2$, C_j will go on detecting H found by C_i, else it will return to the mode before receiving the data. The threshold TH_1 prevents that C_j is on the line $\overleftrightarrow{C_iH}$, and TH_2 prevents C_j is too far from H. The method of detecting H by C_j is as follows.

Let υ denote the plane defined by C_j and $\overleftrightarrow{C_iH}$. So the normal vector of υ is $\boldsymbol{\omega} = \boldsymbol{l}_i \times \overleftrightarrow{C_iC_j}$, namely

$$\boldsymbol{\omega} = \begin{bmatrix} X_{\boldsymbol{\omega}} \\ Y_{\boldsymbol{\omega}} \\ Z_{\boldsymbol{\omega}} \end{bmatrix} = \begin{bmatrix} Y_{\boldsymbol{l}_i}(Z_{C_i} - Z_{C_j}) - Z_{\boldsymbol{l}_i}(Y_{C_i} - Y_{C_j}) \\ Z_{\boldsymbol{l}_i}(X_{C_i} - X_{C_j}) - X_{\boldsymbol{l}_i}(Z_{C_i} - Z_{C_j}) \\ X_{\boldsymbol{l}_i}(Y_{C_i} - Y_{C_j}) - Y_{\boldsymbol{l}_i}(X_{C_i} - X_{C_j}) \end{bmatrix} \quad (6)$$

Because υ passes C_j and H, it is a 2D detecting problem that C_j finds H in υ (Fig.2). C_j need control the horizontal and vertical angle of optical axis, namely β_j^h and β_j^v, to achieve the purpose mentioned above. The direction vector of the optical axis $\overleftrightarrow{C_jo}$ is denoted as $\boldsymbol{l}_j$, if $\overleftrightarrow{C_jo}$ is in υ, then $\boldsymbol{l}_j \perp \boldsymbol{\omega}$, so

$$\boldsymbol{l}_j \cdot \boldsymbol{\omega} = 0 \quad (7)$$

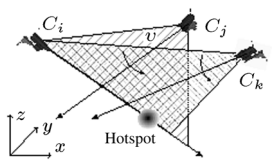

Fig. 2. Cooperatively detect and locate hotspot

So from Eqs.(5) $\sim$ (7), the relationship between β_j^h and β_j^v can be obtained as follows:

$$\beta_j^v = \arctan\frac{X\boldsymbol{\omega}\cos\beta_j^h + Y\boldsymbol{\omega}\sin\beta_j^h}{Z\boldsymbol{\omega}} \tag{8}$$

C_j will control β_j^h and β_j^v according to above relationship to detect H in plane υ.

2. Optimal estimated location of the hotspot

The camera C_i transmits data to cameras around, and then these cameras start to detect the hotspot with the above method. If C_j finds a hotspot H'', it will calculate the straight line, $\overleftrightarrow{C_jH''}$, which passes C_j and the hotspot with Eqs.(1) $\sim$ (5), and then transmits a set of data to C_i. The data includes $P(C_j)$, the direction vector of $\overleftrightarrow{C_jH''}$ and the intersection of $\overleftrightarrow{C_jH''}$ and $\overleftrightarrow{C_iH}$. If $\overleftrightarrow{C_jH''}$ and $\overleftrightarrow{C_iH}$ don't intersect, the intersection is de?ned as the point that is the intersection of their common perpendicular and $\overleftrightarrow{C_iH}$. If C_j finds two or more hotspots, it will transmit all the data of these hotspots to C_i. However only one of them is H, and others will generate 'phantom' hotspots. C_i will receive sets of data from some cameras and some intersections are generated on $\overleftrightarrow{C_iH}$. In normal case, the straight lines intersecting $\overleftrightarrow{C_iH}$ at H are more than the ones intersecting at a 'phantom' hotspot. On other words, the intersections related to H are more, and they are closer apart. So two intersections between which the distance is shortest are the most possible points related to H. We assume they are the intersections of $\overleftrightarrow{C_iH}$ and two lines ($\overleftrightarrow{C_jH}$ and $\overleftrightarrow{C_kH}$). Then the node C_i starts to calculate the world coordinates of H with the three lines, namely $\overleftrightarrow{C_iH}$, $\overleftrightarrow{C_jH}$ and $\overleftrightarrow{C_kH}$, and the other cameras will go on searching other hotspots.

The method of calculating the coordinates with three lines is provided as following. Usually, the intersection point of these lines is the center of H. However, these lines cannot intersect at a point because of error and noise in practice. Thus, the next step is to estimate $P(H)$. Let $\|Q, \overleftrightarrow{AB}\|$ denote the distance from the point Q to the straight line $\overleftrightarrow{AB}$. We assume H is approximate to the point H' which can minimize $\sum_{n=i,j,k}\|H', \overleftrightarrow{C_nH}\|$. For convenience in calculation, we estimate $P(H')$ with the following procedures.

We assume two points, Q_i and Q_j, are a pair of closest points which are on $\overleftrightarrow{C_iH}$ and $\overleftrightarrow{C_jH}$, respectively. In other words, Q_i and Q_j are the intersections of the common perpendicular of $\overleftrightarrow{C_iH}$ and $\overleftrightarrow{C_jH}$. So

$$\begin{cases} (P(Q_i) - P(Q_j)) \cdot \boldsymbol{v}_i = 0 \\ (P(Q_i) - P(Q_j)) \cdot \boldsymbol{v}_j = 0 \end{cases} \tag{9}$$

where $P(Q_i) = P(C_i) + \|C_i, Q_i\| \cdot \boldsymbol{v}_i$, $P(Q_j) = P(C_j) + \|C_j, Q_j\| \cdot \boldsymbol{v}_j$, $\boldsymbol{v}_i$ and $\boldsymbol{v}_j$ are the direction vectors of $\overleftrightarrow{C_iH}$ and $\overleftrightarrow{C_jH}$. We can obtain the coordinates of Q_i and Q_j by solving Eq.(9). They are

$$\begin{cases} P(Q_i) = (P(C_j) - P(C_i)) \cdot [(\boldsymbol{v}_j \cdot \boldsymbol{v}_i)\boldsymbol{v}_j - (\boldsymbol{v}_j \cdot \boldsymbol{v}_j)\boldsymbol{v}_i] \\ \qquad\qquad \cdot \boldsymbol{v}_i / [(\boldsymbol{v}_i \cdot \boldsymbol{v}_j)^2 - (\boldsymbol{v}_i \cdot \boldsymbol{v}_i)(\boldsymbol{v}_j \cdot \boldsymbol{v}_j)] + P(C_i), \\ P(Q_j) = (P(C_i) - P(C_j)) \cdot [(\boldsymbol{v}_i \cdot \boldsymbol{v}_j)\boldsymbol{v}_i - (\boldsymbol{v}_i \cdot \boldsymbol{v}_i)\boldsymbol{v}_j] \\ \qquad\qquad \cdot \boldsymbol{v}_j / [(\boldsymbol{v}_j \cdot \boldsymbol{v}_i)^2 - (\boldsymbol{v}_j \cdot \boldsymbol{v}_j)(\boldsymbol{v}_i \cdot \boldsymbol{v}_i)] + P(C_j) \end{cases}$$

The coordinates of the midpoint for Q_i and Q_j, denoted as $Q_{i,j}$ is

$$P(Q_{i,j}) = (P(Q_i) + P(Q_j))/2.$$

If there are only two thermal cameras C_i and C_j, we can consider $Q_{i,j}$ as the center of H. However two cameras bring a big error to the coordinates. If the error is too big, actors cannot cool the hottest area. Since there are multiple thermal cameras in the TCN, three cameras are used to improve precision of measurement which has been proved by experiments below. If three cameras find the hotspot, we can obtain 3 points $Q_{i,j}$, $Q_{j,k}$ and $Q_{k,i}$, from lines $\overleftrightarrow{C_iH}$, $\overleftrightarrow{C_jH}$ and $\overleftrightarrow{C_kH}$. Then we consider the incenter, namely the center of the inscribed circle, of the triangle $\Delta Q_{i,j}Q_{j,k}Q_{k,i}$ as the point H'. So that

$$\begin{aligned} P(H') =& [P(Q_{i,j})\ P(Q_{j,k})\ P(Q_{k,i})] \\ & \times [\|Q_{j,k}, Q_{k,i}\|\|Q_{k,i}, Q_{i,j}\|\|Q_{i,j}, Q_{j,k}\|]^T \\ & /(\|Q_{j,k}, Q_{k,i}\| + \|Q_{k,i}, Q_{i,j}\| + \|Q_{i,j}, Q_{j,k}\|) \end{aligned}$$

So far, the world coordinates of H has been estimated in 3D space.

IV. Simulation Results

In this section we present detailed experimental evaluation of location of TCNs. We use MATLAB to simulate a TCN detecting and locating in a data center. The range of the data center is 20m×20m×2m. Four thermal camera nodes are deployed at the ceiling corners. All the nodes can pan and tilt automatically, and the rotation angles are known. The maximum error of rotation angles is 0.5°. The parameters of the thermal cameras are that $F = 50$mm, $\alpha^h = 36°$ and $\alpha^v = 27°$. The size of thermal images is 320 × 240 pixels. Each image pixel provides temperature data, and the accuracy is ±2°C. We design several experiments to examine the performance of the TCN.

1. Experiment 1

To compare the performance of the proposed TCN, we also simulate other location system with the same parameters and errors. The one consists of 2 thermal cameras deployed sparsely and the other consists of a pair of adjacent thermal cameras at the spacing of 20cm.

We generate randomly hotspots to test. In order to prevent the shapes of the hotspots affecting estimation of hotspots centers in thermal images, we test 6 types of hotspots which are: 1. "sphere", 2. "horizontal cylinder", 3. "vertical cylinder", 4. "horizontal plan", 5. "vertical plane", 6. "random". All of their volumes are same. The number of every type of hotspots is 100, total is 600.

We use error distance to evaluate the accuracy which is the distance between the real location and estimated location of the hotspot. Fig.3 illustrates the average error distances generated by the TCN, two cameras deployed sparsely and a pair of adjacent cameras. We can conclude that the TCN has the best accuracy because of usage of more cameras. Generating error is due to several factors, such as the error of rotation angles and the error of temperature detectors. The factor that most influence the accuracy is estimating hotspot center in the thermal image. Since the hotspot center in the thermal image

is not a clear point like a corner in a visible image, estimating location of the center in a thermal image can bring inevitable error.

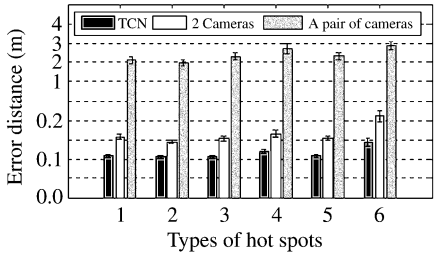

Fig. 3. Location accuracies of different systems via the type of hotspots

2. Experiment 2

The distances between cameras and hotspots can affect the resolution of hotspots in thermal images, so that they can affect locating. Thus we design this experiment to evaluate accuracy of locating everywhere hotspots.

At first, we use C_1, C_2 and C_3 of four cameras to cooperatively detect and locate everywhere hotspots. Fig.4(a) illustrates the location of cameras and the distribution of error distances at floor, middle and ceiling layer. We can find accuracy changes with location of the hotspots. The worst accuracies occur at two edges of the floor layer. According to this result, we obtain the distribution of accuracy of using any 3 cameras. Thus we make the second test. We use four cameras to detect and locate cooperatively. Every hotspot is located two times. The detailed process is as followed. If a hotspot is located by any 3 cameras, according to the locating result, the second locating is done using the set of 3 cameras of which accuracy at this location is best. The distribution of accuracy of the second locating is illustrated in Fig.4(b). The accuracy is improved by one order of magnitude.

3. Experiment 3

Because cameras cannot zoom, cameras cannot resize hotspots in images. This experiment is designed to examine the effect of volume change of hotspots on accuracy. We generate 10 sets of hotspots at volumes of spheres with diameters from 0.2m to 1.1m. Every set consists of 6 types of 100 hotspots.

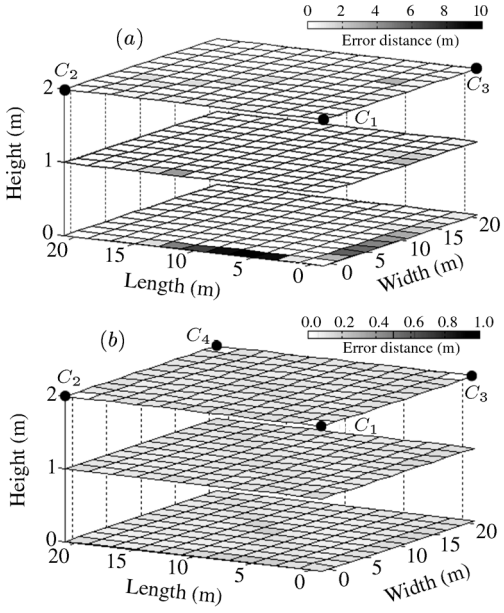

Fig. 4. Error distances of using 3 or 4 cameras to locate hotspots at three layers

Fig.5 illustrates the error distances in locating hotspots of different volumes. We can find error distance increases with increasing volume. The reason is that cameras cannot obtain the integral hotspot in the thermal images if the volume is too big. So that coordinates of the hotspot center in the image is estimated inaccurately. All these cases finally cause increase in the error distance. Two methods can resolve this problem. The first is that we choose cameras which can obtain the integral hotspot to locate. However implement of this method need more cameras. The second is that warning temperature is adaptively controlled to redefine hotspots. This method requires warning temperature defined in the cameras which locate the same hotspot must be equal.

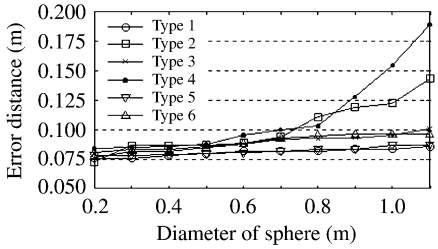

Fig. 5. Error distances in locating hotspots of different volumes

V. Conclusion

We present a TCN which includes multiple thermal cameras and actors. It can be used in large data centers to detect, locate and cool hotspots cooperatively. We mainly solved cooperatively detecting and locating hotspots with the TCN. Accuracy in locating the hotspot have great influence on cooling it by actors. Since a TCN contains multiple thermal cameras, we proposed to locate a hotspot by three cameras. Experiments proved three cameras located more accurately than two cameras. In the future, we will estimate more information of hotspots to grade them according to influence.

References

[1] E. Samadiani, Y. Joshi and F. Mistree, "The thermal design of a next generation data center: A conceptual exposition", *Journal of Electronic Packaging*, Vol.130, No.4, pp.041104, 2008.

[2] J. Moore, J.S. Chase and P. Ranganathan, "Weatherman: Automated, online and predictive thermal mapping and management for data centers", *Proc. of IEEE Autonomic Computing* (*ICAC*), Dublin, Ireland, pp.155–164, 2006.

[3] A.J. Shah, V.P. Carey, C.E. Bash and C.D. Patel, "Exergy analysis of data center thermal management systems", *Journal of Heat Transfer*, Vol.130, No.2, pp.021401, 2008.

[4] S. McAllister, V.P. Carey, A. Shah, C. Bash and C. Patel, "Strategies for effective use of exergy-based modeling of data center thermal management systems", *Microelectronics Journal*, Vol.39, No.7, pp.1023–1029, 2008.

[5] J. Loper, S. Parr, "Energy efficiency in data centers: A new policy frontier", *Environmental Quality Management*, Vol.16, No.4, pp.83–97, 2007.

[6] Q. Tang, S.K.S. Gupta and G. Varsamopoulos, "Energy-efficient thermal-aware task scheduling for homogeneous high-performance computing data centers: A cyber-physical approach", *IEEE Trans. Parallel and Distributed Systems*, Vol.19, No.11, pp.1458–1472, 2008.

[7] C. Bash and G. Forman, "Cool job allocation: Measuring the power savings of placing jobs at cooling-efficient locations in the data center", *Proc. of the USENIX Annual Technical Conference* (*ATC*), Berkeley, USA, pp.1–6, 2007.

[8] T. Heath, A.P. Centeno, P. George, L. Ramos, Y. Jaluria and R. Bianchini, "Mercury and freon: Temperature emulation and management for server systems", *Proc. of Architectural Support for Programming Languages and Operating Systems* (*ASPLOS*), San Jose, USA, pp.106–116, 2006.

[9] I.F. Akyildiz, I.H. Kasimoglu, "Wireless sensor and actor networks: Research challenges", *Ad Hoc Networks* (*Elsevier*), Vol.2, No.4, pp.351–367, 2004.

[10] T. Melodia, D. Pompili, V.C. Gungor and I.F. Akyildiz, "Communication and coordination in wireless sensor and actor networks", *IEEE Trans. Mobile Computing*, Vol.6, No.10, pp.1116–1129, 2007.

[11] T. Mukherjee, A. Banerjee, G. Varsamopoulos, S.K.S. Gupta and S. Rungta, "Spatio-temporal thermal-aware job scheduling to minimize energy consumption in virtualized heterogeneous data centers", *Computer Networks*, Vol.53, No.17, pp.2888–2904, 2009.

[12] B. Zhang, Y. Luo, X. Wang, Z. Wang, Y. Sun, H. Chen, Z. Xu and X. Li, "Whole-system live migration mechanism for virtual machines", *Acta Electronica Sinica*, Vol.37, No.4, pp.894–899, 2009. (in Chinese)

LIU Hang received B.S. degree in 2004, and is pursuing the Ph.D. degree in the School of Information and Communication Engineering, Dalian University of Technology, China. From Nov. 2008 to Dec. 2009, he is a visiting researcher in the Department of Electrical and Computer Engineering, the State University of New Jersey, Rutgers, USA. His main research interests are in image processing and wireless multimedia sensor networks.

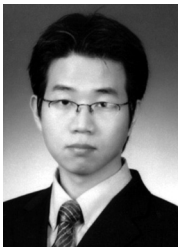

LEE Eun Kyung is pursuing Ph.D. degree in the Department of Electrical and Computer Engineering, the State University of New Jersey since Feb. 2009. He received M.S. degree in Electrical and Computer Engineering in Jan. 2009. His research interests include ad hoc and sensor networks, cross-layer protocol, and network optimization and control.

POMPILI Dario is an Assistant Professor with the Department of Electrical and Computer Engineering, the State University of New Jersey, USA. He received "laurea" summa cum laude in Telecommunications Engineering, Italy in 2001, and the Ph.D. degree in System Engineering in 2004, from the University of Rome "La Sapienza". He received second Ph.D. degree in Electrical and Computer Engineering at the Broadband and Wireless Networking Laboratory, Georgia Institute of Technology, Atlanta, USA, under the guidance of Dr. Ian F. Akyildiz. His main research interests are in underwater acoustic sensor networks, wireless sensor and actor networks, and satellite networks.

KONG Xiangwei is currently a professor and vice director of Research Center of Multimedia Information Processing and Security of Dalian University of Technology, China. During 2006–2007, she was a visiting scholar of Purdue University, USA. Prof. Kong is a member of signal processing society of IEEE. From 2004–2009, she is a vice director of multimedia information security branch of Chinese Institute of Electronics, China. She is also the member of academic committee of China Image and Graphic Association, China. Now, she is a referendary of IEEE Trans. Systems, Man and Cybernetics, Pattern Recognition, Fuzzy and System, Journal of Information and Computational Science and Acta Electronica Sinica *etc.* Her research contributions encompass aspects of multimedia information security, digital watermarking, digital image forensics, image and signal processing and wireless sensor networks.